Outline

- Introduction, principles
- Method n°1 : Demons
- Evaluation
- Method n°2 : B-Splines
- Method n°3 : Deep-learning registration
- **Method n°4 : TPS (Thin Plate Spline)**
- The « sliding » problem
- Spatio-temporal deformable registration
- Conclusion

Thin-Plate Spline

- Given corresponding source and target points
- Computes a spatial deformation function for every point in the 2D plane or 3D volume

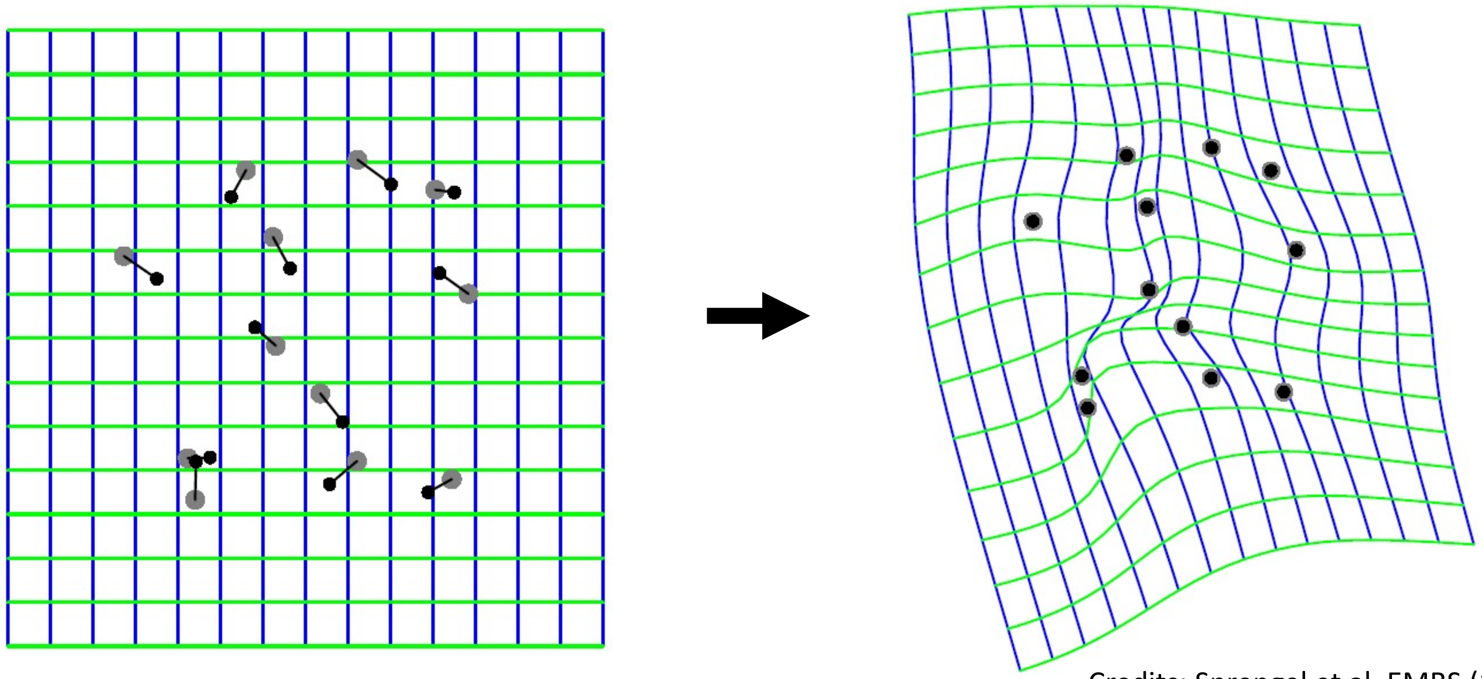

Credits: Sprengel et al, EMBS (1996)

Thin-Plate Spline

Bookstein, Fred L.

"Principal warps: Thin-plate splines and the decomposition of deformations. »

IEEE Transactions on pattern analysis and machine intelligence 11.6 (1989): 567-585.

IEEE TRANSACTIONS ON PATTERN ANALYSIS AND MACHINE INTELLIGENCE, VOL. 11, NO. 6, JUNE 1989 567

Principal Warps: Thin-Plate Splines and the Decomposition of Deformations

FRED L. BOOKSTEIN

Abstract—One conventional tool for interpolating surfaces over scattered data, the *thin-plate spline*, has an elegant algebra expressing the dependence of the physical bending energy of a thin metal plate on point constraints. For interpolation of a surface over a fixed set of nodes in the plane, the bending energy is a quadratic form in the heights assigned to the surface. The spline is the superposition of eigenvectors of the bending energy matrix, of successively larger physical scales, over a tilted flat plane having no bending energy at all.

When these splines are paired, one representing the x-coordinate of another form and the other the y-coordinate, they aid greatly in the modeling of biological shape change as *deformation*. In this context, the pair becomes an interpolation map from R^2 to R^2 relating two sets of *landmark points*. The spline maps decompose, in the same way as the spline surfaces, into a linear part (an affine transformation) together with the superposition of *principal warps*, which are geometrically independent, affine-free deformations of progressively smaller geometrical scales. The warps decompose an empirical deformation into orthogonal features more or less as a conventional orthogonal functional analysis decomposes the single scene. This paper demonstrates the decomposition of deformations by principal warps, extends the method to deal with curving edges between landmarks, relates this formalism to other applications of splines current in computer vision, and indicates how they might aid in the extraction of features for analysis, comparison, and diagnosis of biological and medical images.

Index Terms—Affine transformations, biharmonic equation, biomedical image analysis, deformation, principal warps, quadratic variation, shape, thin-plate splines, warping.

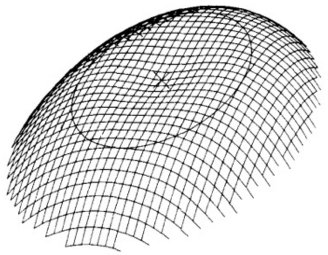

Fig. 1. Fundamental solution of the biharmonic equation: a circular fragment of the surface $z(x, y) = -r^2 \log r^2$ viewed from above. The X is at $(0, 0, 0)$; the remaining zeros of the function are on the circle of radius 1 drawn.

circle, where $r = 1$. The maximum of the surface is achieved all along a circle of radius $1/\sqrt{e} \sim 0.607$ concentric with the circle of radius 1 that is drawn.

The function $U(r)$ satisfies the equation

$$\Delta^2 U = \left(\frac{\partial^2}{\partial x^2} + \frac{\partial^2}{\partial y^2}\right)^2 U \propto \delta_{(0,0)}.$$

The right-hand side of this expression is proportional to

Thin-Plate Spline

Rohr, Karl, et al.

"Landmark-based elastic registration using approximating thin-plate splines."

IEEE Transactions on medical imaging 20.6 (2001): 526-534.

526 IEEE TRANSACTIONS ON MEDICAL IMAGING, VOL. 20, NO. 6 JUNE2001

Landmark-Based Elastic Registration Using Approximating Thin-Plate Splines

K. Rohr*, H. S. Stiehl, R. Sprengel, T. M. Buzug, J. Weese, and M. H. Kuhn

***Abstract*—We consider elastic image registration based on a set of corresponding anatomical point landmarks and approximating thin-plate splines. This approach is an extension of the original interpolating thin-plate spline approach and allows to take into account landmark localization errors. The extension is important for clinical applications since landmark extraction is always prone to error. Our approach is based on a minimizing functional and can cope with isotropic as well as anisotropic landmark errors. In particular, in the latter case it is possible to include different types of landmarks, e.g., unique point landmarks as well as arbitrary edge points. Also, the scheme is general with respect to the image dimension and the order of smoothness of the underlying functional. Optimal affine transformations as well as interpolating thin-plate splines are special cases of this scheme. To localize landmarks we**

steps: 1) extraction of landmarks in the different datasets; 2) establishing the correspondence between the landmarks; and 3) computing the transformation between the datasets using the information from 1) and 2). Among the different types of landmarks (points, lines, surfaces, and volumes) we here consider point landmarks.

Previous work on point-based elastic registration has concentrated on a) selecting the corresponding landmarks manually and on b) using an interpolating transformation model (e.g., [2], [7], and [11]). The basic approach draws upon thin-plate splines or other splines and is computationally efficient. However, an interpolation scheme forces the corresponding landmarks to ex-

Thin-Plate Spline

- A minimization problem
  - Minimizing distances between source and target points
  - Minimizing distortion of the space
    (as if bending a thin sheet of metal)

- There is a closed-form solution
  - Solving a linear system of equations

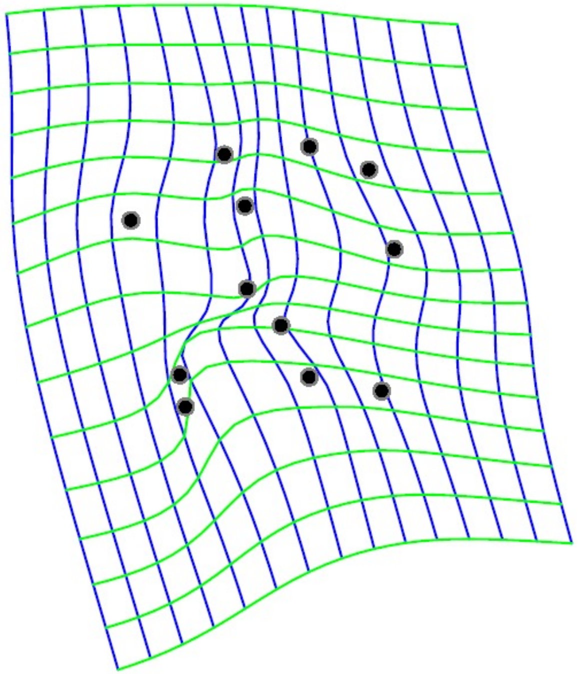

Thin-Plate Spline

- Input
  - Source points: $p_1,\ldots,p_n$
  - Target points: $q_1,\ldots,q_n$
- Output
  - A deformation function f[p] for any point p

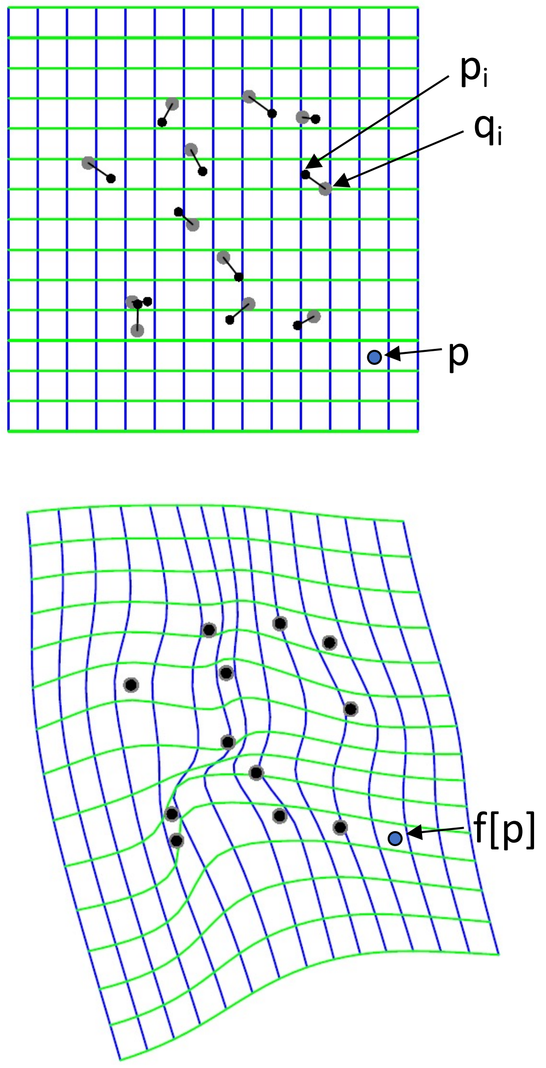

Thin-Plate Spline

- Minimization formulation

$$E = E_f + \lambda E_d$$

  - E_f: fitting term
    Measures how close is the deformed source to the target
  - E_d: distortion term
    Measures how much the space is warped
  - λ : weight
    Controls how much non-rigid warping is allowed

Thin-Plate Spline

- Fitting term
  - Minimizing sum of squared distances between deformed source points and target points

$$E_f = \sum_{i=1}^{n} \| f[p_i] - q_i \|^2$$

Thin-Plate Spline

- Distortion term
  - Minimizing a physical bending energy on a metal sheet (2D):

$$E_d = \iint \left(\left(\frac{\partial^2 f}{\partial x^2} \right)^2 + 2 \left(\frac{\partial^2 f}{\partial x y} \right)^2 + \left(\frac{\partial^2 f}{\partial y^2} \right)^2 \right)^2 dx\, dy$$

  - The energy is zero when the deformation is affine
    - Translation, rotation, scaling, shearing

Thin-Plate Spline

- Finding the minimizer for $\mathbf{E} = \mathbf{E}_f + \lambda \mathbf{E}_d$
  - Uniquely exists, and has a closed form:

$$f[p] = M \cdot p + \sum_{i=1}^{n} \phi[\|p - p_i\|]\, v_i$$

where $\phi[r] = r^2 \operatorname{Log}[r]$

λ

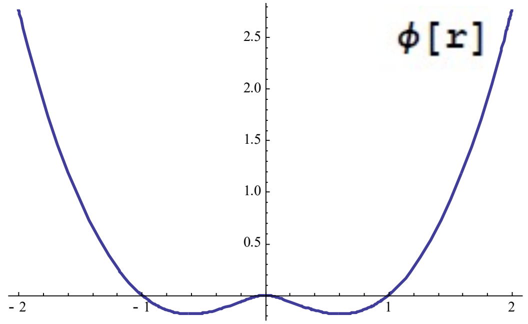

- M: an affine transformation matrix
- Expressed as a RBF phi
- v_i: coefficients
- Both M and v_i are determined by p_i,q_i,

$$E_{tps,smooth}(f) = \sum_{i=1}^{K} \|y_i - f(x_i)\|^2 + \lambda \iint \left[\left(\frac{\partial^2 f}{\partial x_1^2} \right)^2 + 2 \left(\frac{\partial^2 f}{\partial x_1 \partial x_2} \right)^2 + \left(\frac{\partial^2 f}{\partial x_2^2} \right)^2 \right] \mathrm{d}x_1 \, \mathrm{d}x_2$$

$$f_{tps}(z, \alpha) = f_{tps}(z, d, c) = z \cdot d + \sum_{i=1}^{K} \phi(\|z - x_i\|) \cdot c_i$$

$$x_i \longrightarrow X$$

$$y_i \longrightarrow Y$$

$$\phi(\|x_i - x_j\|) \longrightarrow \Phi \; (K \times K)$$

$$X = [Q_1 | Q_2] \begin{pmatrix} R \\ 0 \end{pmatrix}$$

$$\boxed{\begin{aligned} \hat{c} &= Q_2 (Q_2^T \Phi Q_2 + \lambda I_{(k-D-1)})^{-1} Q_2^T Y \\ \hat{d} &= R^{-1} Q_1^T (Y - \Phi \hat{c}) \end{aligned}}$$

Thin-Plate Spline

- Result
  - At higher λ , the deformation is closer to an affine transformation

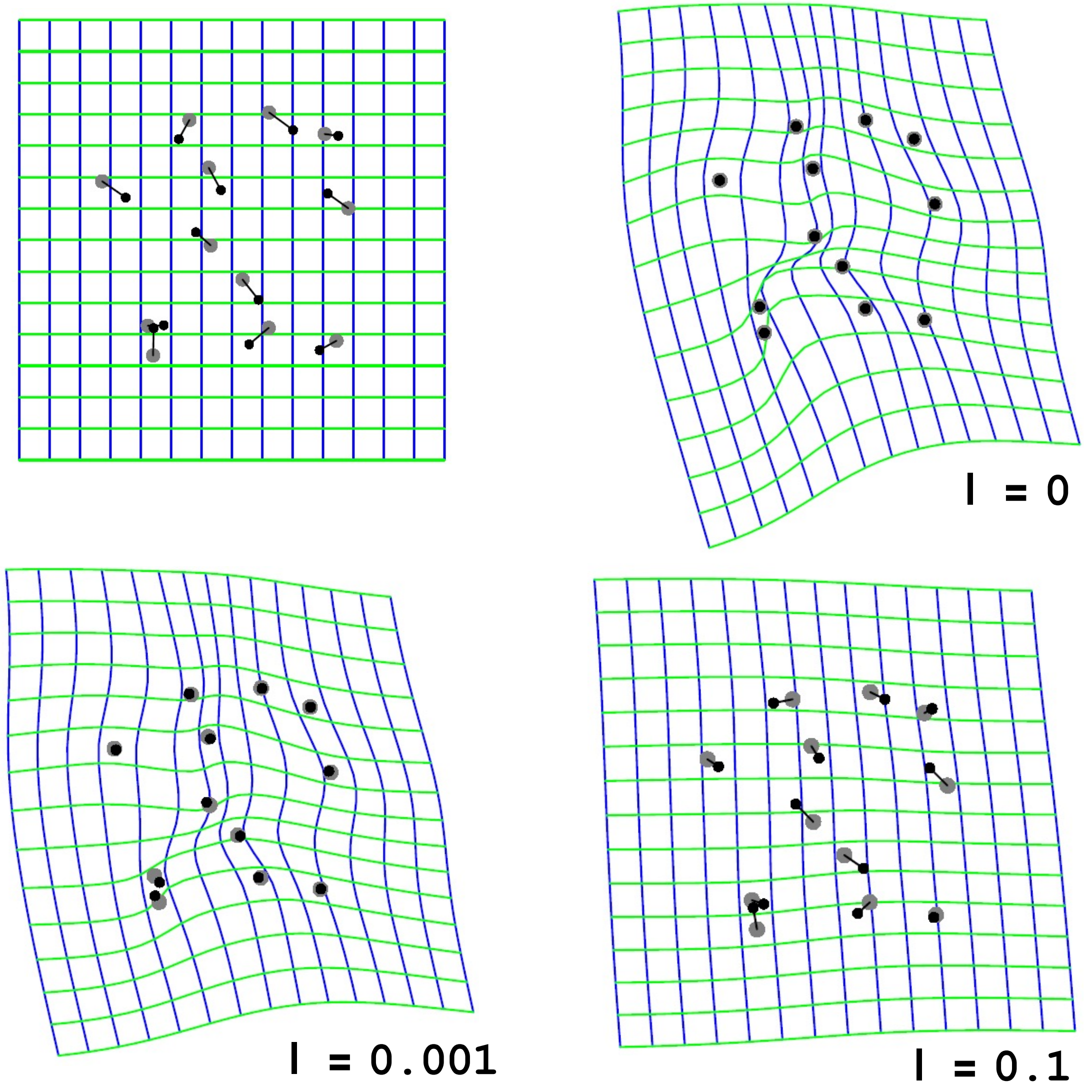

Credits: Sprengel et al, EMBS (1996)

Thin-Plate Spline

- Application: image registration
  - Manual or automatic feature pair detection

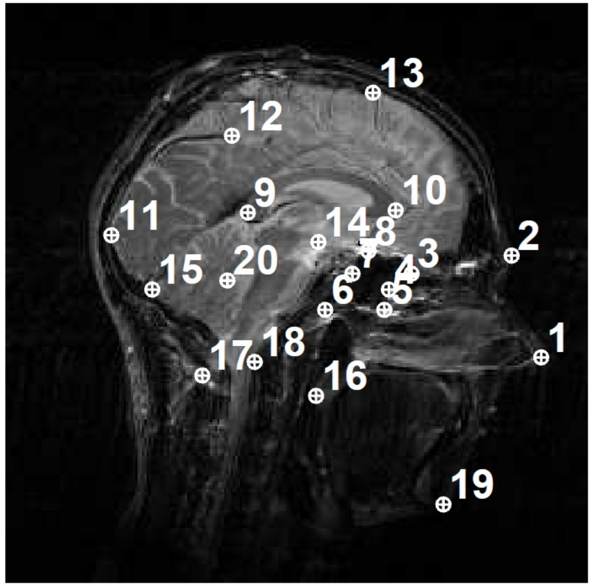

Source

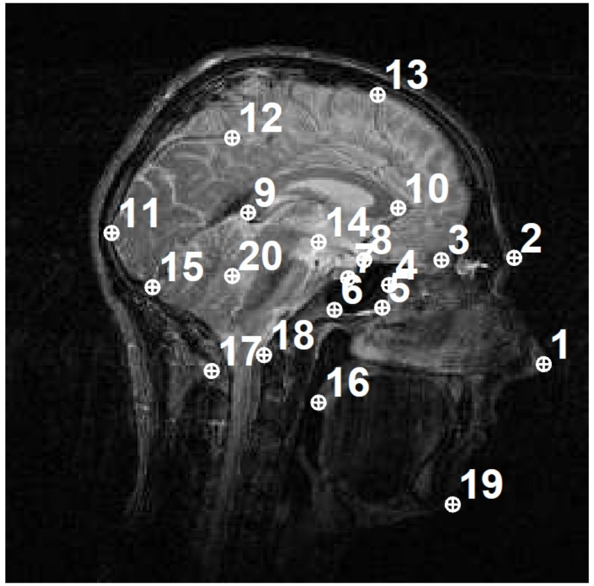

Target

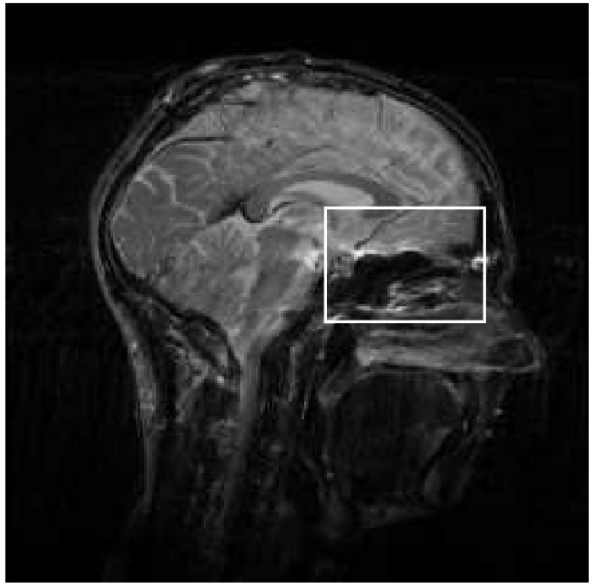

Deformed source

Credits: Rohr et al, TMI (2001)

Thin-Plate Spline

- Advantages
  - Smooth deformations, with physical analogy
  - Closed-form solution
  - Few free parameters (no tuning is required)

- Disadvantages
  - Solving the equations still takes time
    (hence cannot perform “interactive” deformation)

SIFT

- Example of automated point corresponding landmarks detection

- SIFT : Scale Invariant Feature Transform
  Lowe, David G. (1999). "Proceedings of the International Conference on Computer Vision" 2. pp. 1150–1157

2 steps:

- **Identify** points with “special” characteristic (gradient, scale-invariant) in both image
- **Pair** image points with criteria

Outline

- Introduction, principles
- Method n°1 : Demons
- Evaluation
- Method n°2 : B-Splines
- Method n°3 : Deep-learning registration
- Method n°4 : TPS (Thin Plate Spline)
- **The « sliding » problem**
- Spatio-temporal deformable registration
- Conclusion

The “sliding problem”

- Deformable registration is **ill-posed**
- Requires prior knowledge

- Smoothness is a common prior
- Sliding causes discontinuity in the motion field: leads to errors

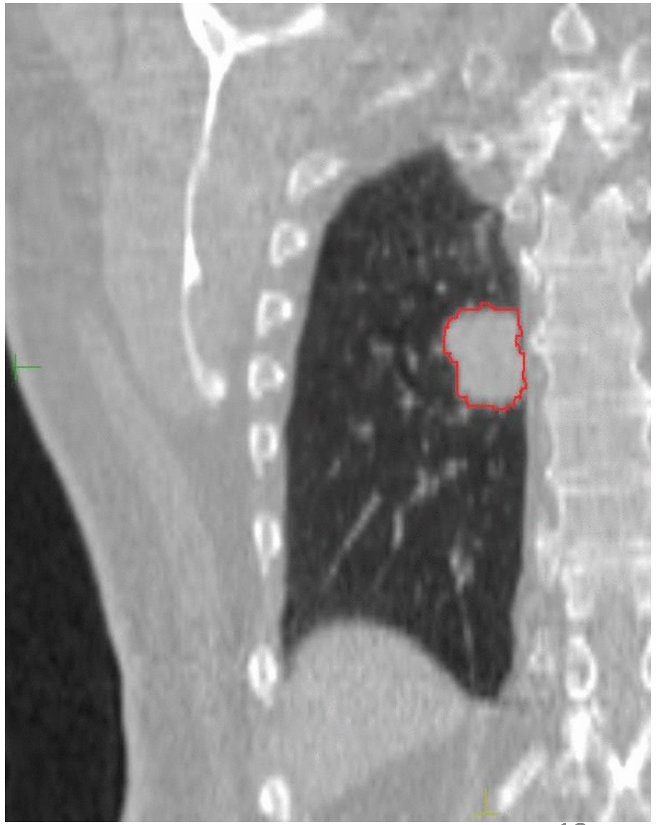

Previous work

- Biomechanical modelling
  - Contact surface problem solved with FEM
  - [Villard et al 2005] [Al-Mayah et al 2008]

- Adapted regularization
  - [Wolthaus et al 2008] [Ruan et al 2008]

- Approach by “masks”
  - [Wu et al 2008] [Werner et al 2009] [Kabus et al 2009]

Main principles

- Provide interface where sliding occurs
- Decompose registration spatially
- Separate moving from less-moving regions: **motion mask**

- Segmentation:
  - Not anatomical
  - Based on geometry
  - We used level sets

- Perform 2 registrations

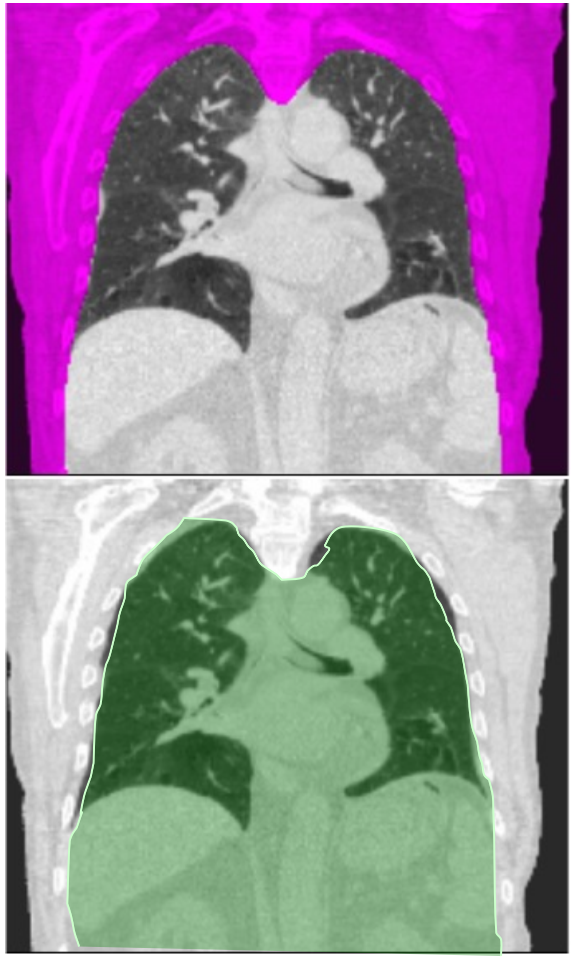

Extract some anatomical structures

- Lungs, bones and body extraction
- Filtering, mathematical morphology and region growing *[Perona and Malik, 1990; van Rikxoort et al., 2009]*

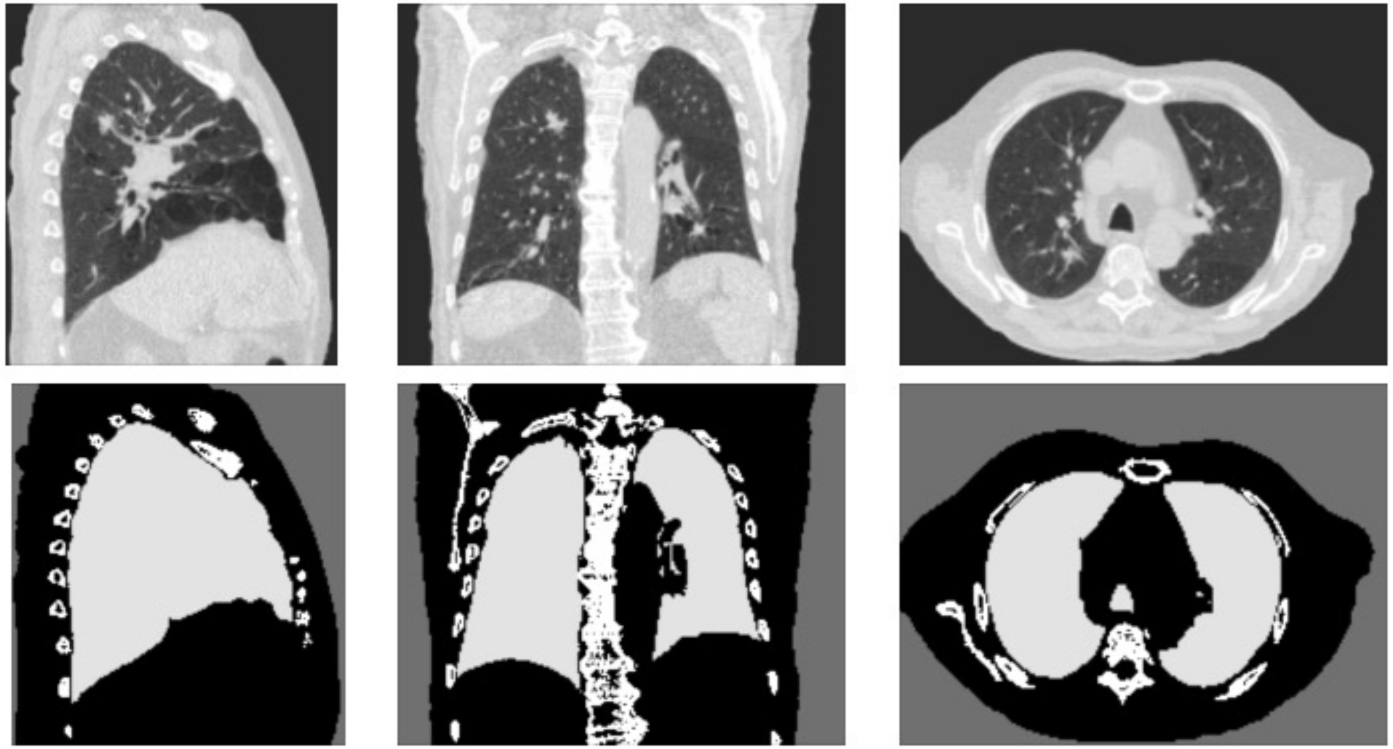

Filling the abdomen, monitor the air

Results

- Mask allows to enforce stronger smoothness
- Accuracy significantly improved for 5 patients of 6

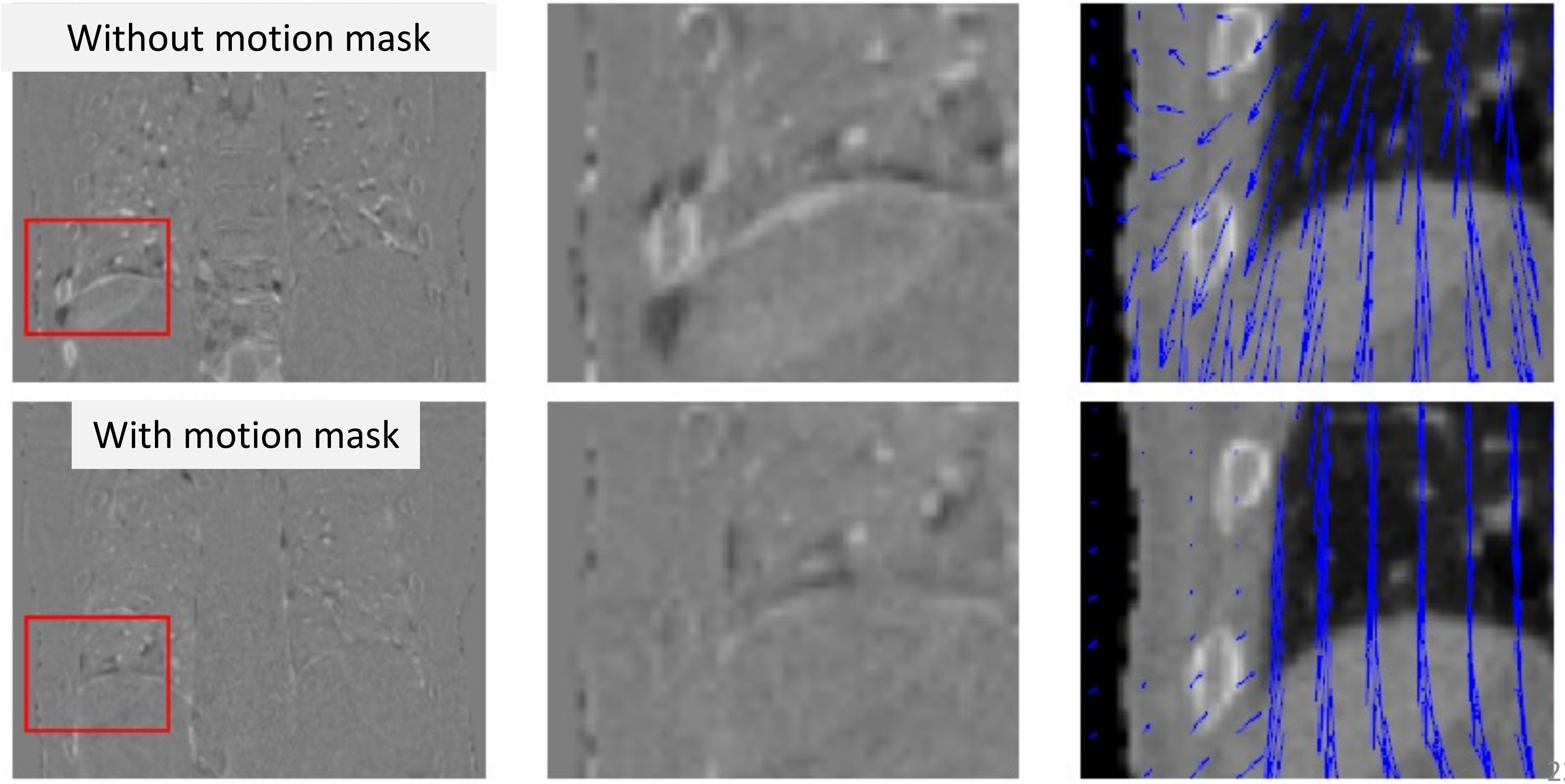

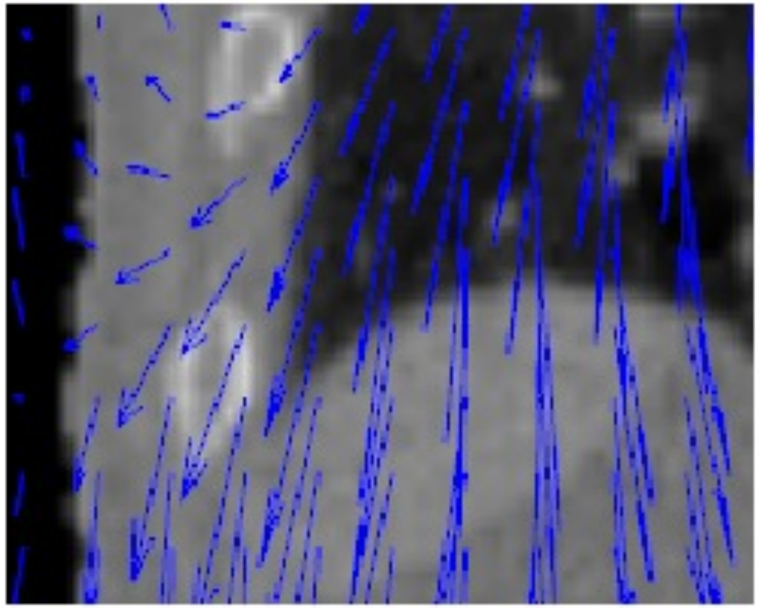

Single region registration

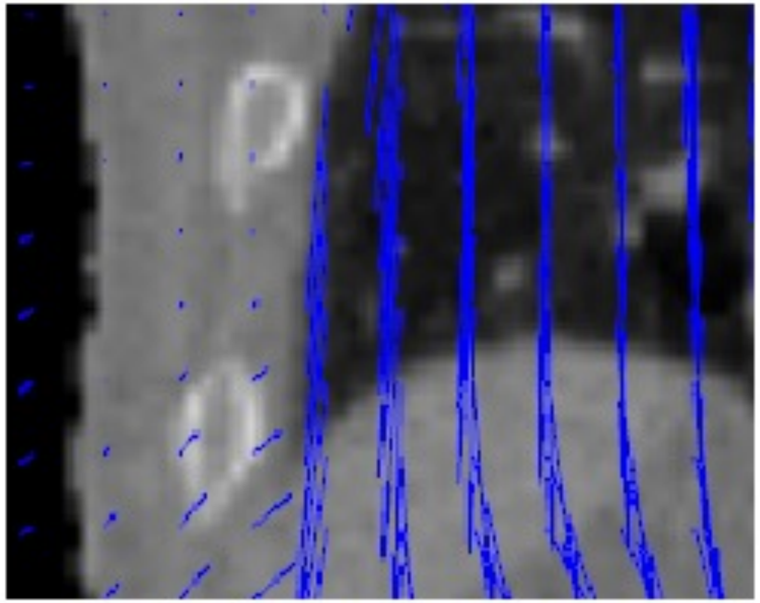

Two regions registration

Results

Estimate registration accuracy based on 600 landmarks

TRE

Patient	Before (mm)	No Mask (mm)	Mask (mm)
1	9.4	2.4	1.8
2	7.3	2.8	2.6
3	7.1	1.8	1.6
4	6.7	1.6	1.5
5	14.0	2.8	1.8
6	6.8	2.1	1.9
Mean	**8.6**	**2.3**	**1.9**

Use this mask in DIR ?

- Solution n°1 : perform two registration independently

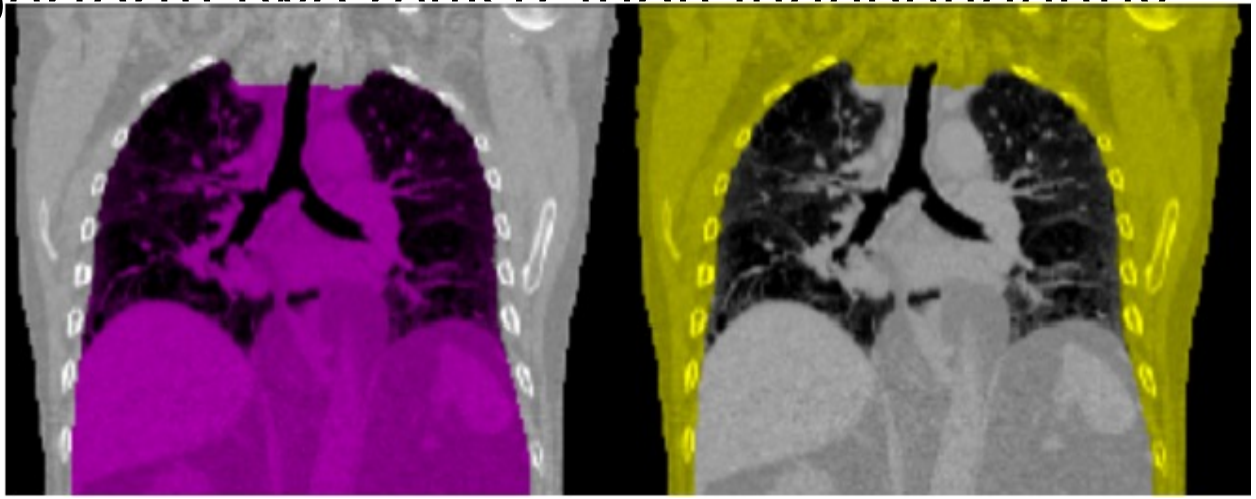

- But :

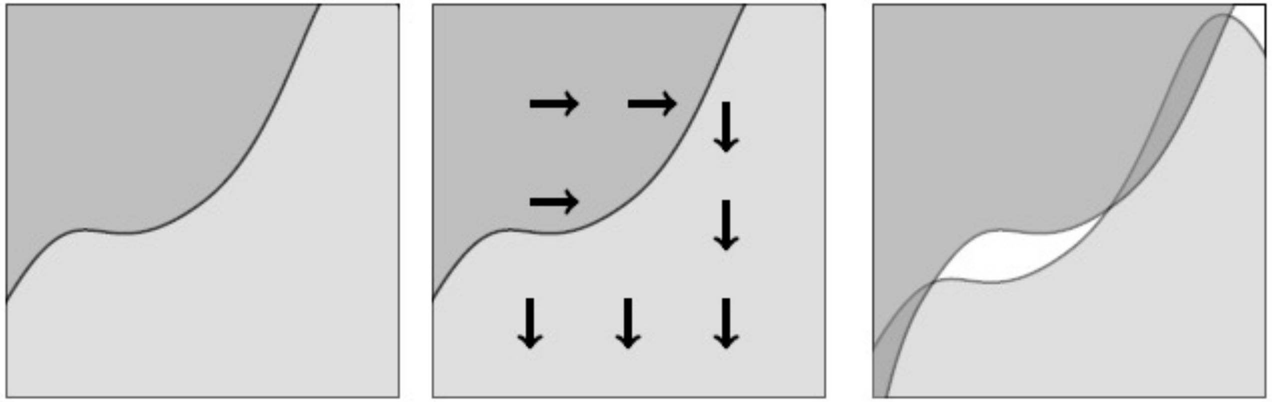

(a) Labels (b) Vector field (c) Forward warp

Use this mask in DIR ?

- Solution n°2 :
  - Direction-Dependent Regularization
  - Consider directions normal/tangential to the boundaries
  - [Schmidt-Richberg et al., 2009] : for non-parametric DIR
  - [Delmon et a. 2013] : for parametric B-Splines

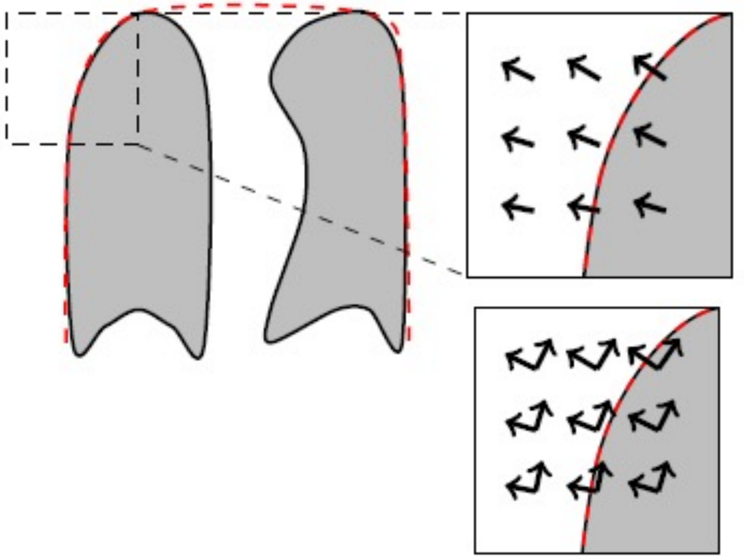

Use this mask in DIR ?

- Solution n°2 :
  - Direction-Dependent Regularization
  - Consider directions normal/tangential to the boundaries
  - [Schmidt-Richberg et al., 2009] : for non-parametric DIR
  - [Delmon et a. 2013] : for parametric

Inside

$$\boldsymbol{T}(x) = \sum_i \boldsymbol{c_i}\beta_i(x)$$

Normal direction

$$\boldsymbol{T}(x) = \begin{cases} \boldsymbol{B^N}(x) + \boldsymbol{B^{\Omega}}(x) & \text{if } x \in \Omega, \\ \boldsymbol{B^N}(x) + \boldsymbol{B^{\overline{\Omega}}}(x) & \text{if } x \in \overline{\Omega}. \end{cases}$$

Outside

$$\boxed{\begin{aligned} \boldsymbol{c_i^N} &= p_i^N \boldsymbol{N}(i) \\ \boldsymbol{c_i^{\Omega}} &= p_i^{\Omega,U}\boldsymbol{U}(i) + p_i^{\Omega,V}\boldsymbol{V}(i) \\ \boldsymbol{c_i^{\overline{\Omega}}} &= p_i^{\overline{\Omega},U}\boldsymbol{U}(i) + p_i^{\overline{\Omega},V}\boldsymbol{V}(i) \end{aligned}}$$

Direction-Dependent Regularization

- Results

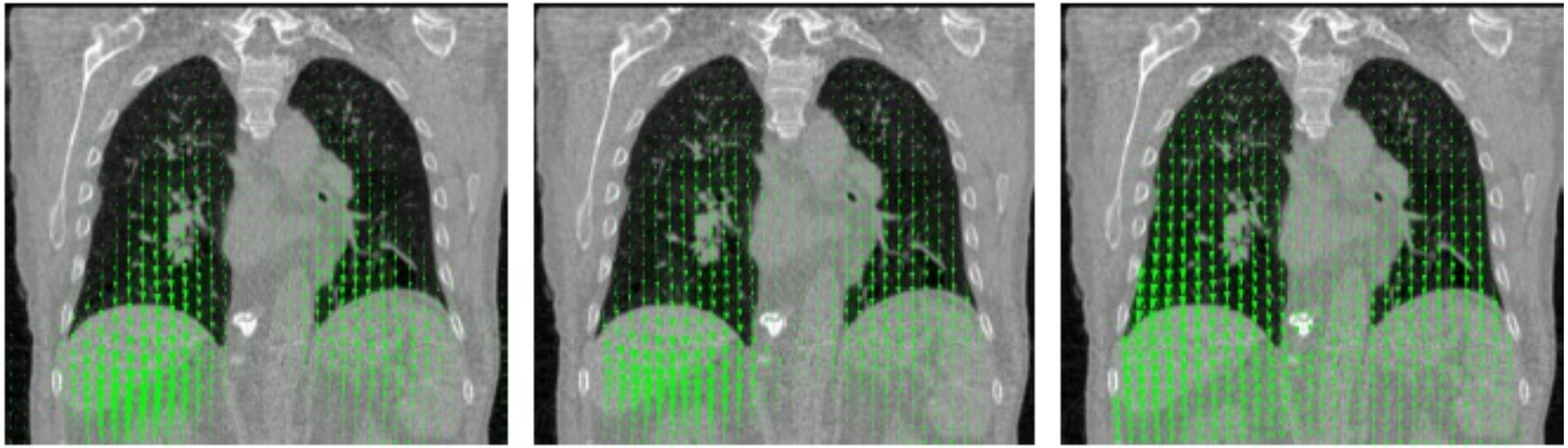

(a) Single region (b) Multiple regions (c) Multiple regions with normal

Direction-Dependent Regularization

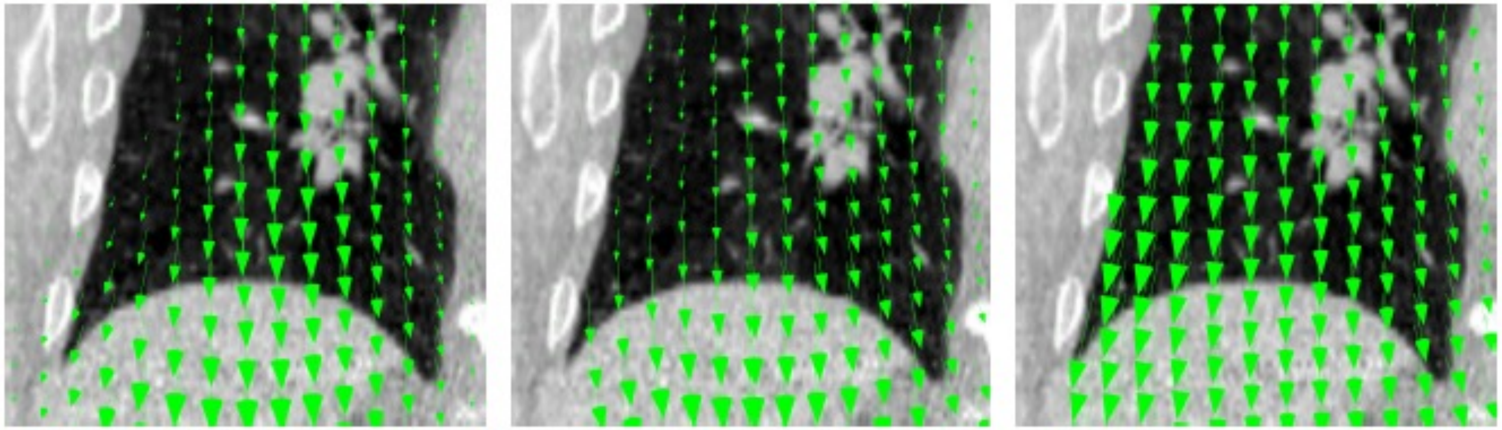

(a) Single region (b) Multiple regions (c) Multiple regions with normal

	Before		Single region		Multi regions		Multi regions with normal	
	Mean	SD	Mean	SD	Mean	SD	Mean	SD
average	8.42	5.64	3.82	4.15	1.42	1.05	1.43	1.06

Direction-Dependent Regularization

	Before		Single region		Multi regions		Multi regions with normal	
	Mean	SD	Mean	SD	Mean	SD	Mean	SD
average	8.42	5.64	3.82	4.15	1.42	1.05	1.43	1.06

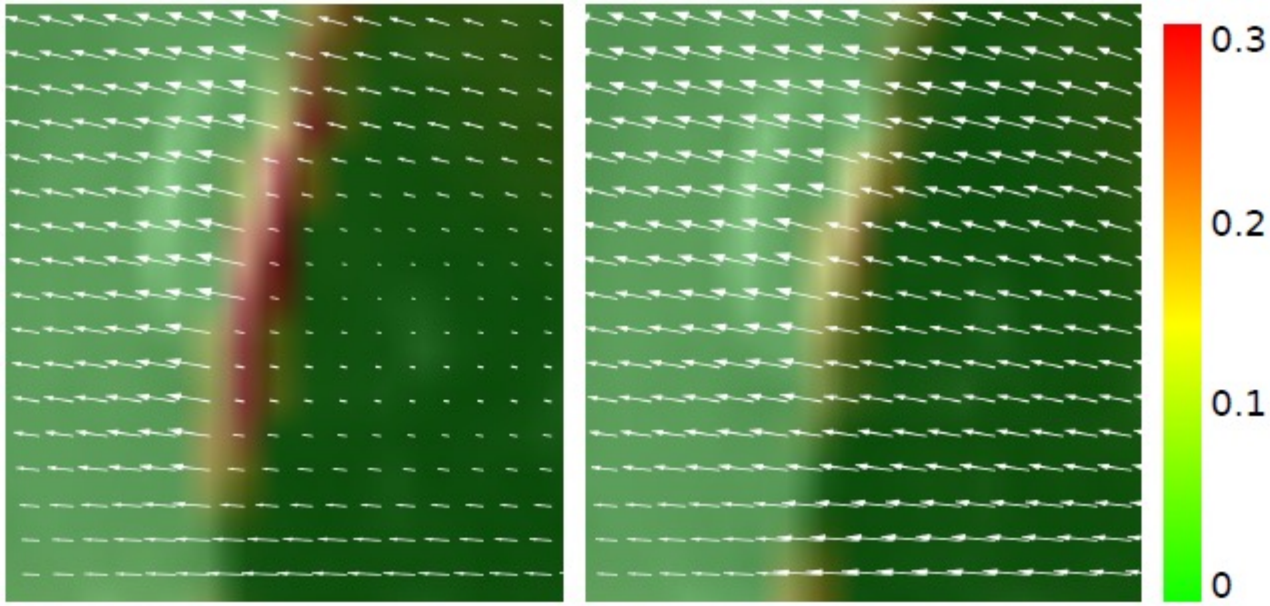

(a) Multiple regions (b) Multiple regions with normal

Figure: A Jacobian based quality measure $|\log(Jac(proj(T(x), \mathbf{N})))|$

Conclusion on motion mask extraction

- Comes down to monitored segmentation of binary images
- Allows to preserve sliding motion in the motion field: it facilitates deformable registration
- Allows to introduce stronger smoothness assumptions: renders the algorithm more efficient and robust, while maintaining accuracy

■ Direction-Dependent Regularization may help to further improve consistency

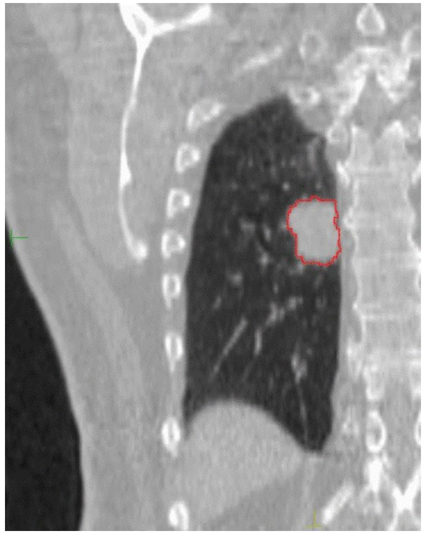

[Vandemeulebroucke et al. Med Phys 2012]

[Delmon et al PMB 2013]

Conclusion – deformable registration

- Numerous applications (not only medical)
- Ill-posed problem (=hard)
- Numerous methods (Demons, B-splines, …)
  no « universal » method
- Validation is difficult

- Notions
  - Geometrical transformation (deformation)
  - Similarity measure
  - Optimisation
  - Validation

Outline

- Introduction, principles
- Method n°1 : Demons
- Evaluation
- Method n°2 : B-Splines
- Method n°3 : Deep-learning registration
- Method n°4 : TPS (Thin Plate Spline)
- The « sliding » problem
- **Spatio-temporal deformable registration**
- Conclusion

4D CT

- Acquisition of 10 volumes 3D (phases)

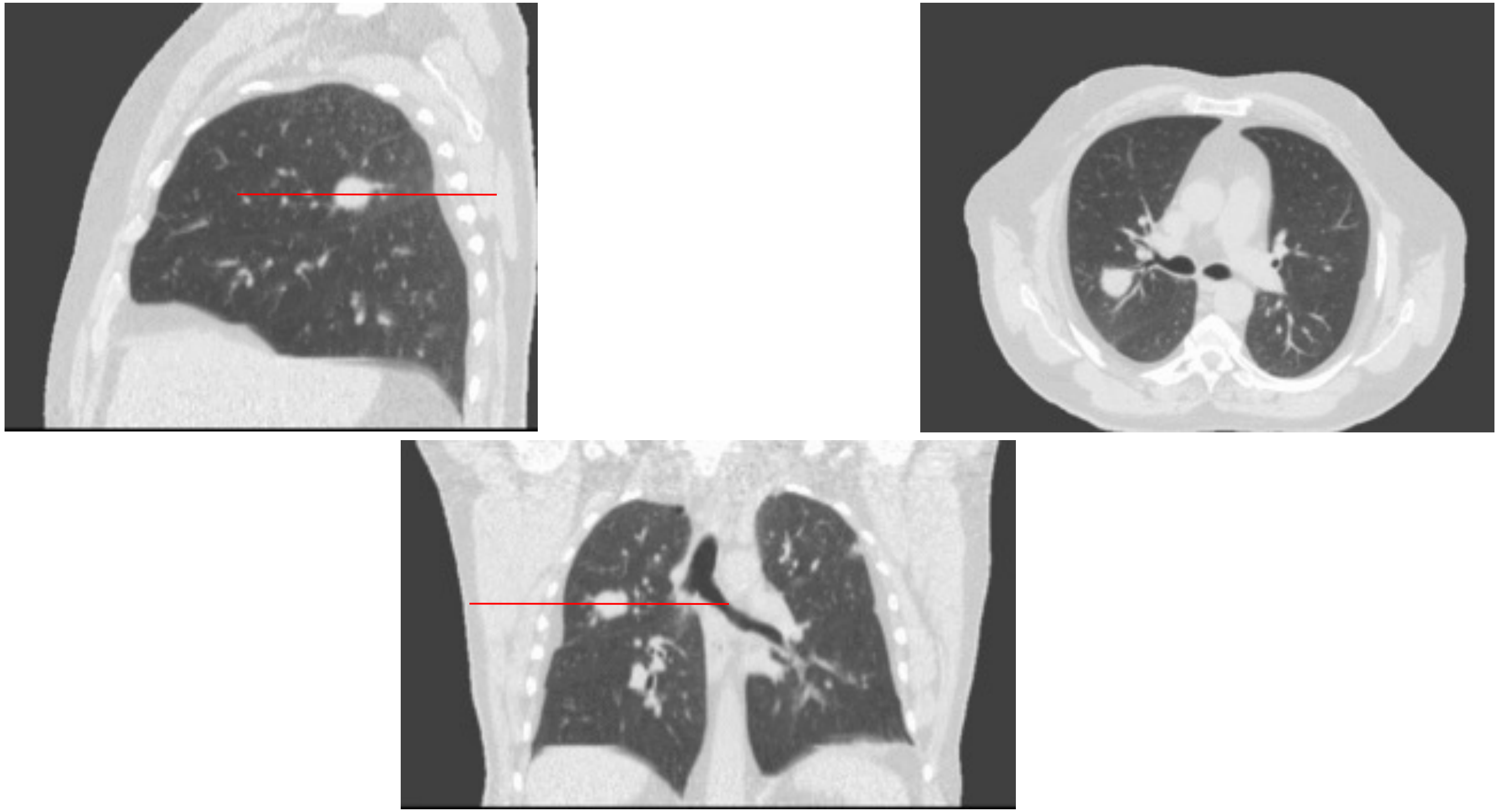

4D CT – breathing motion

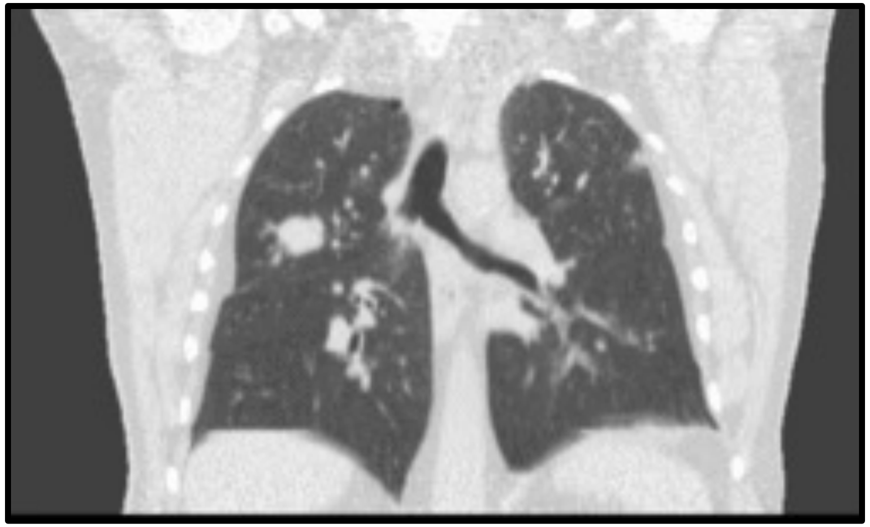

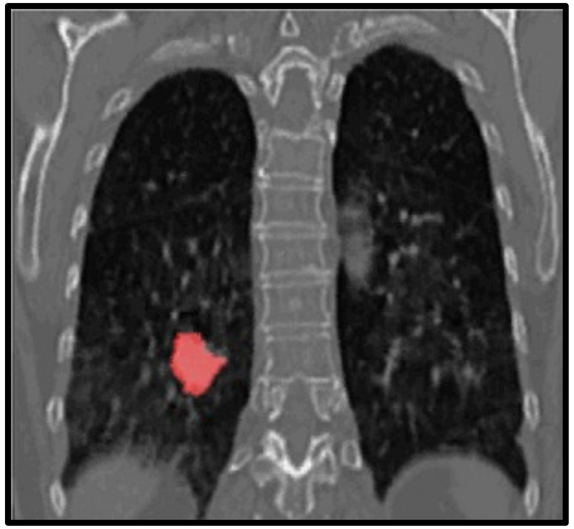

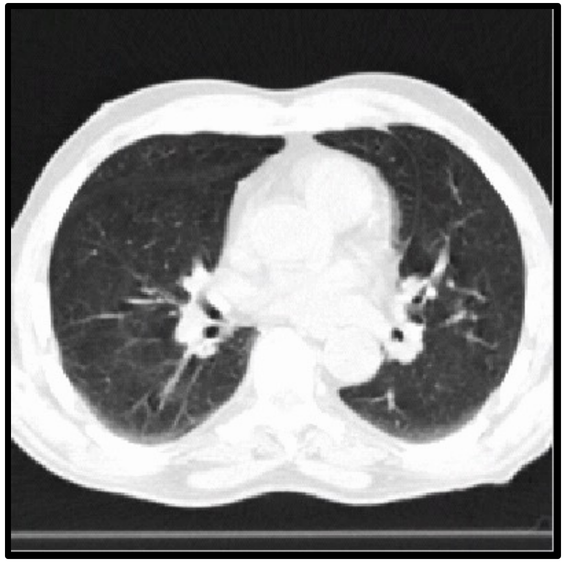

Successive DIR

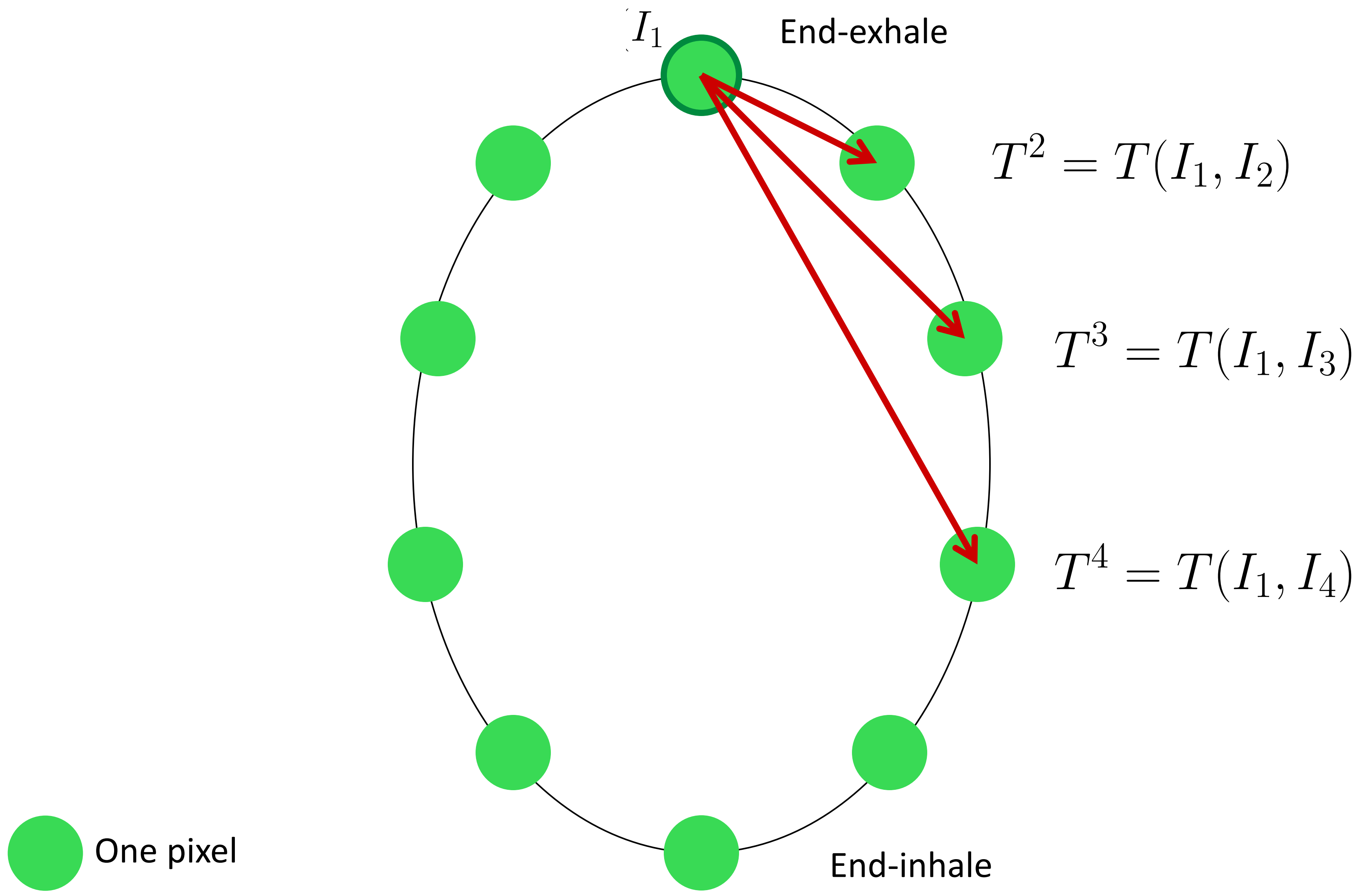

Interpolation between vector fields

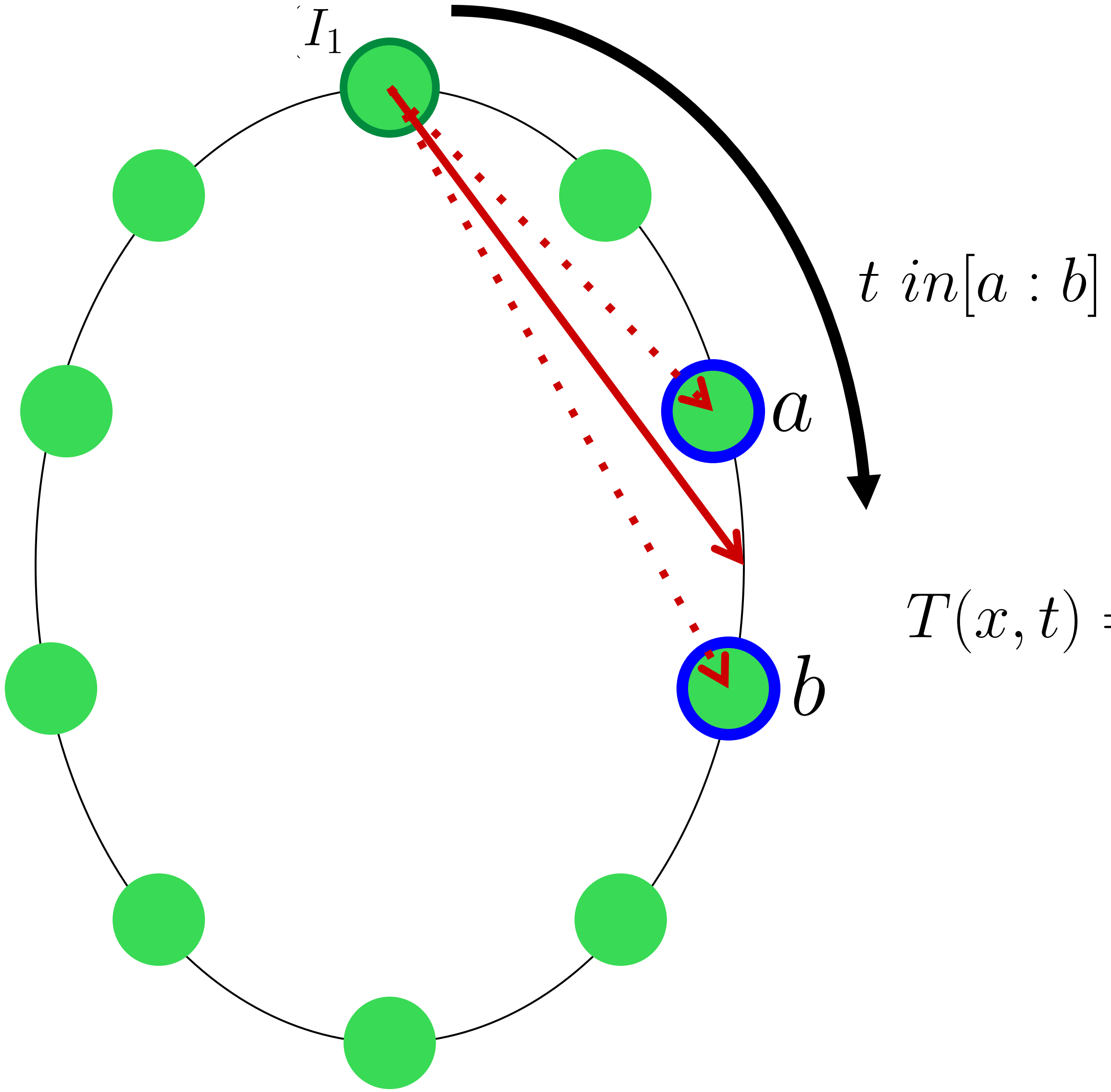

$$T(x,t) = x + \frac{b-t}{b-a}T^a + \frac{t-a}{b-a}T^b$$

DVF : Deformation Vector Field

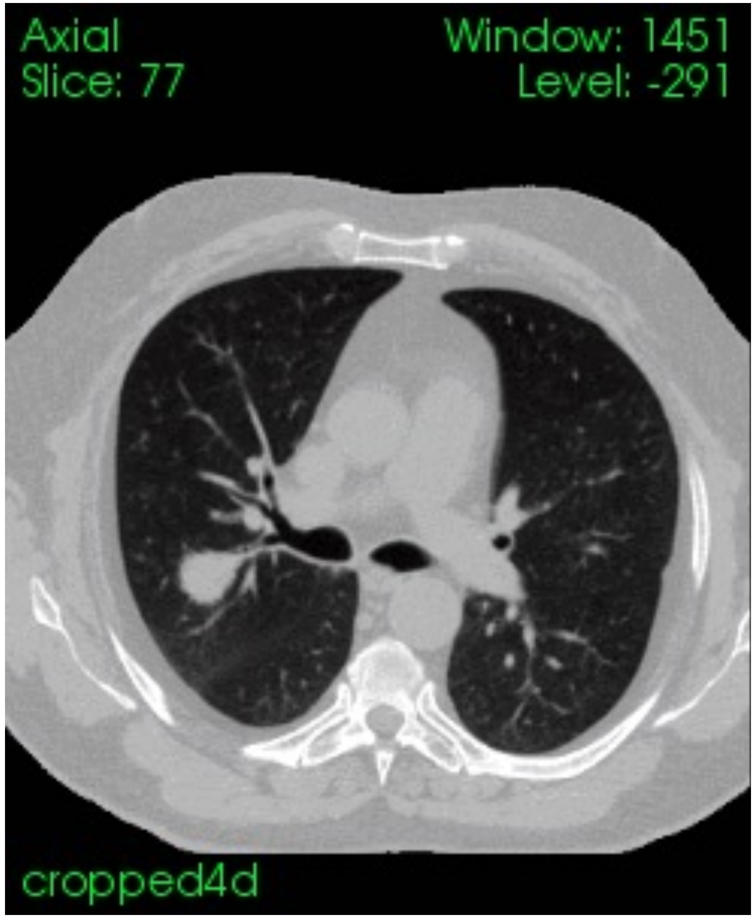

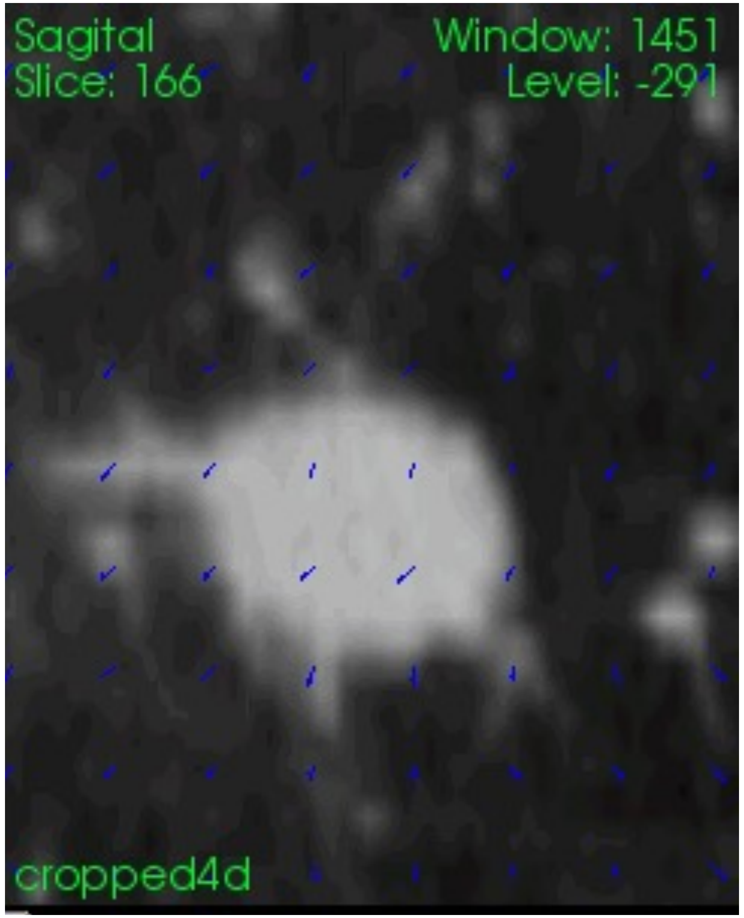

Registration of 4D CT

- 4D registration = register a reference phase to the 9 other phases
- Artifacts: registration can fail locally
- Proposit mporal

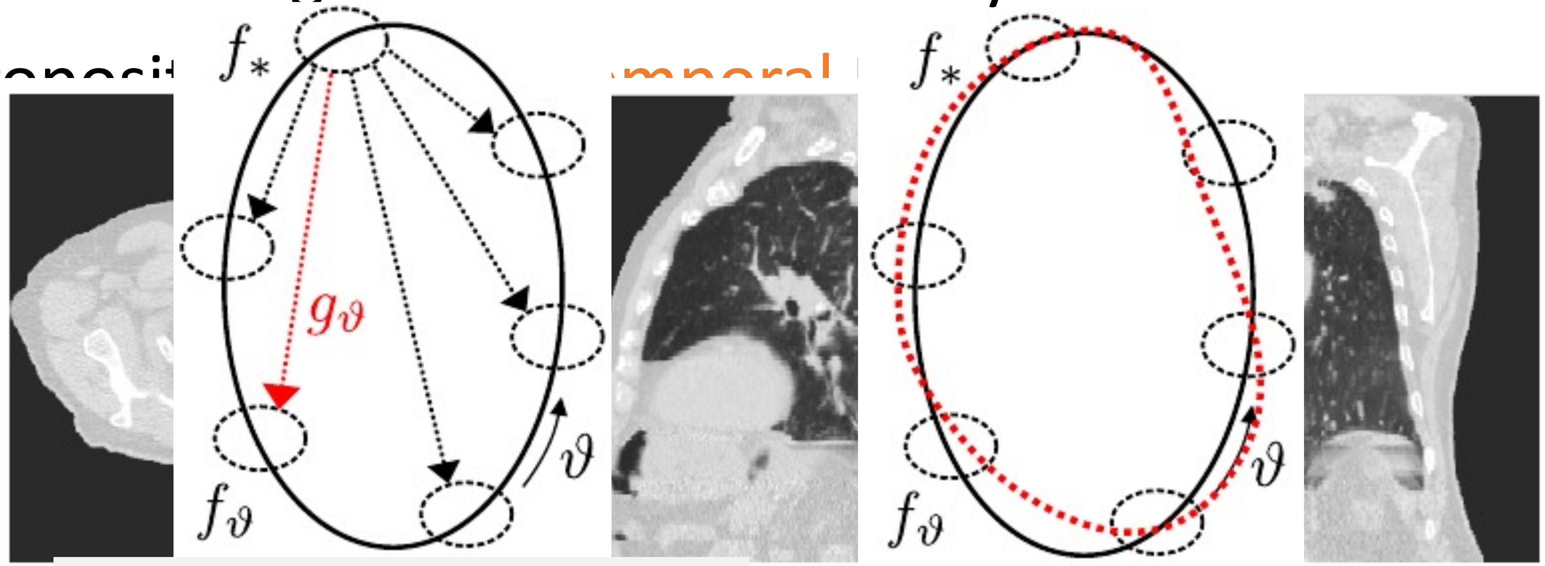

- Consecutive 3D registrations
- Estimating displacements

- Global 4D approach
- Estimating trajectories

Spatio-temporal registration

Previous work

- Spatio-temporal analysis of cardiac motion (Clarysse et al., 2000; Ledesma-Carbayo et al., 2005; Sundar et al., 2009)
- 4D registration of thoracic sequences (Schreibmann et al., 2008)
  - -> No trajectory modelling for respiration
- 3D-4D non-parametric registration (Castillo et al., 2010)
  - -> Trajectory between end-exhale and end-inhale, not cyclic

Our approach

- 3D-4D parametric spatio-temporal registration
  - -> **Cyclic** trajectory covering the whole cycle
  - -> Trajectory modelling specific for **respiration**
  - -> **Compact** a parametrization to improve robustness

Model of trajectory

- Search for plausible trajectories model with as few parameters as possible
- Study trajectories of diaphragm motion of 33 patients (CBCT)
- End up with
  - B-Spline
  - 7 control points (5 DOF)
  - Cyclic
  - Remove smoothness at inhale point

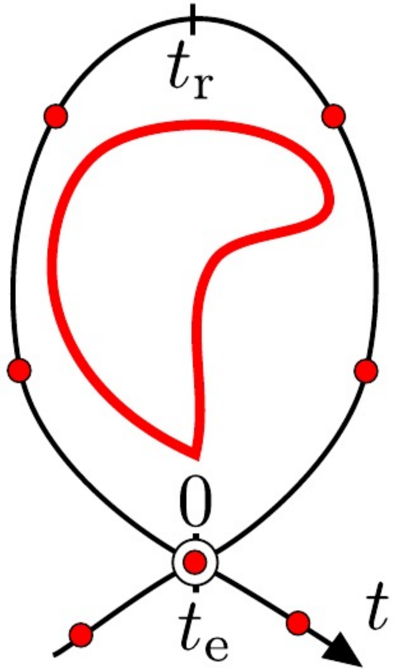

Global 4D DIR

- **Temporal** model $\mathcal{T}_{\mathrm{t}}$ with temporal contraints, e.g. periodicity

$$\left.\begin{array}{l}\mathcal{T}_{\mathrm{t}}(\boldsymbol{x},t)=\boldsymbol{x}+\sum_{l\in\mathbf{L}}\boldsymbol{b}_l\psi_l(t)\\ \mathcal{T}_{\mathrm{t}}(\boldsymbol{x},0)=\mathcal{T}_{\mathrm{t}}(\boldsymbol{x},t_{\mathrm{e}})\end{array}\right\}\Rightarrow \boldsymbol{b}_{l_{\mathrm{e}}}=\sum_{l\in\mathbf{L},l\neq l_{\mathrm{e}}}\boldsymbol{b}_l\frac{\psi_l(0)-\psi_l(t_{\mathrm{e}})}{\psi_{l_{\mathrm{e}}}(t_{\mathrm{e}})}$$

- **Contraints** allow to generate a new set of basis functions ψ_l^{c}

$$\psi_l^{\mathrm{c}}(t)=\psi_l(t)+\frac{\big(\psi_l(0)-\psi_l(t_{\mathrm{e}})\big)\psi_{l_{\mathrm{e}}}(t)}{\psi_{l_{\mathrm{e}}}(t_{\mathrm{e}})}$$

- **Spatial** free-form deformations $\mathcal{T}_{\mathrm{s}}$ (Rueckert et al., 1999)

$$\mathcal{T}_{\mathrm{s}}(\boldsymbol{x})=\boldsymbol{x}+\sum_{\boldsymbol{j}\in\mathbf{J}}\boldsymbol{a}_{\boldsymbol{j}}\phi_{\boldsymbol{j}}(\boldsymbol{x})$$

- Combining $\mathcal{T}_{\mathrm{s}}$ and $\mathcal{T}_{\mathrm{t}}$ gives a **spatio-temporal** model

$$\mathcal{T}_{\mathrm{st}}(\boldsymbol{x},t)=\boldsymbol{x}+\sum_{\boldsymbol{j}\in\mathbf{J}}\sum_{l\in\mathbf{L}^{\mathrm{c}}}\boldsymbol{c}_{\boldsymbol{j},l}\,\phi_{\boldsymbol{j}}(\boldsymbol{x})\psi_l^{\mathrm{c}}(t)$$

Results on simulated artifacts

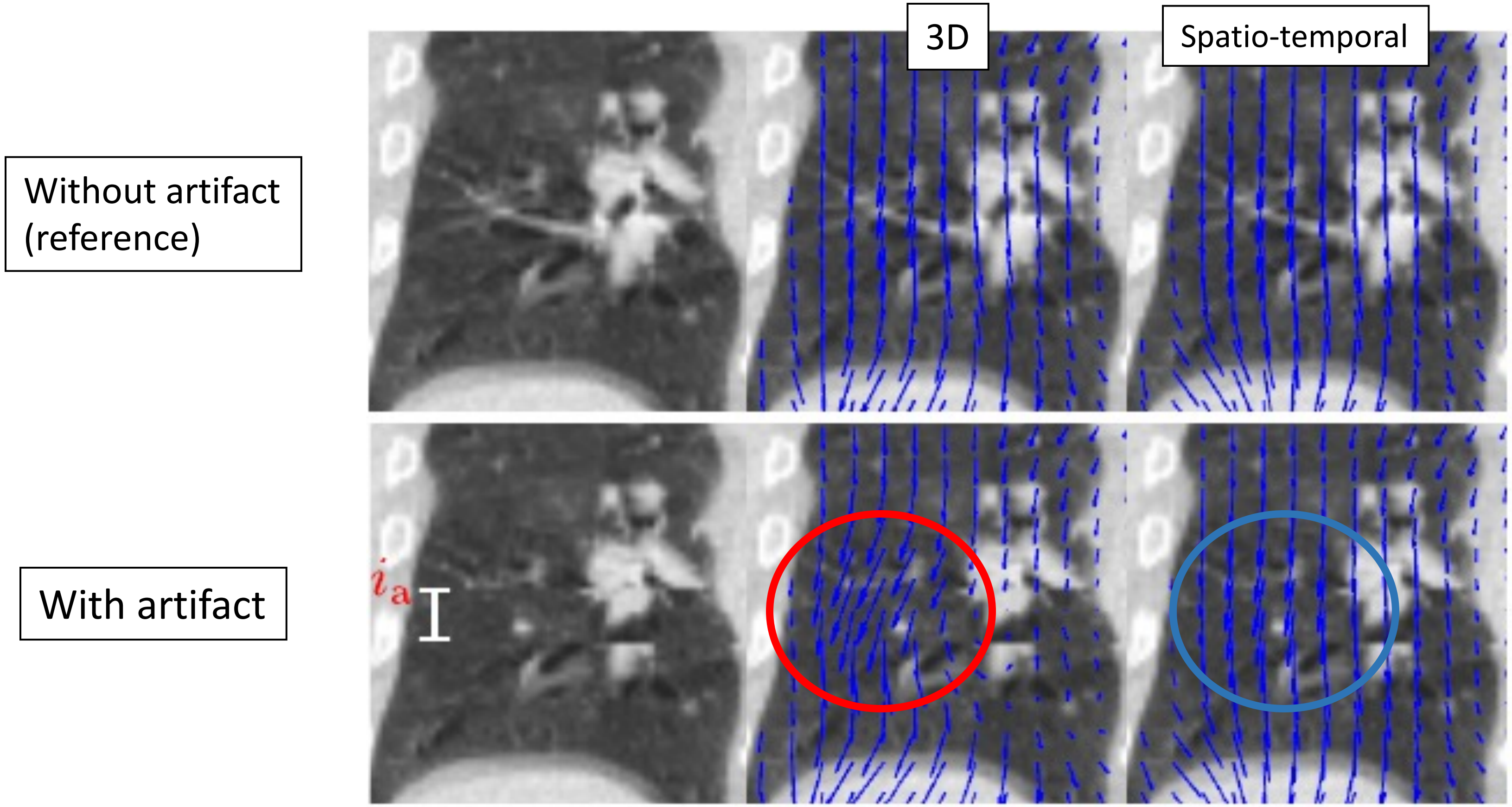

Measure in mm	Initial	3D	Spatio-temporal
Global	9 (3.9)	3.2 (3.4)	1.5 (1.2)
Close to artifact	11.4 (3.7)	**6.8** (4.3)	**1.9** (1.2)

Results on real images

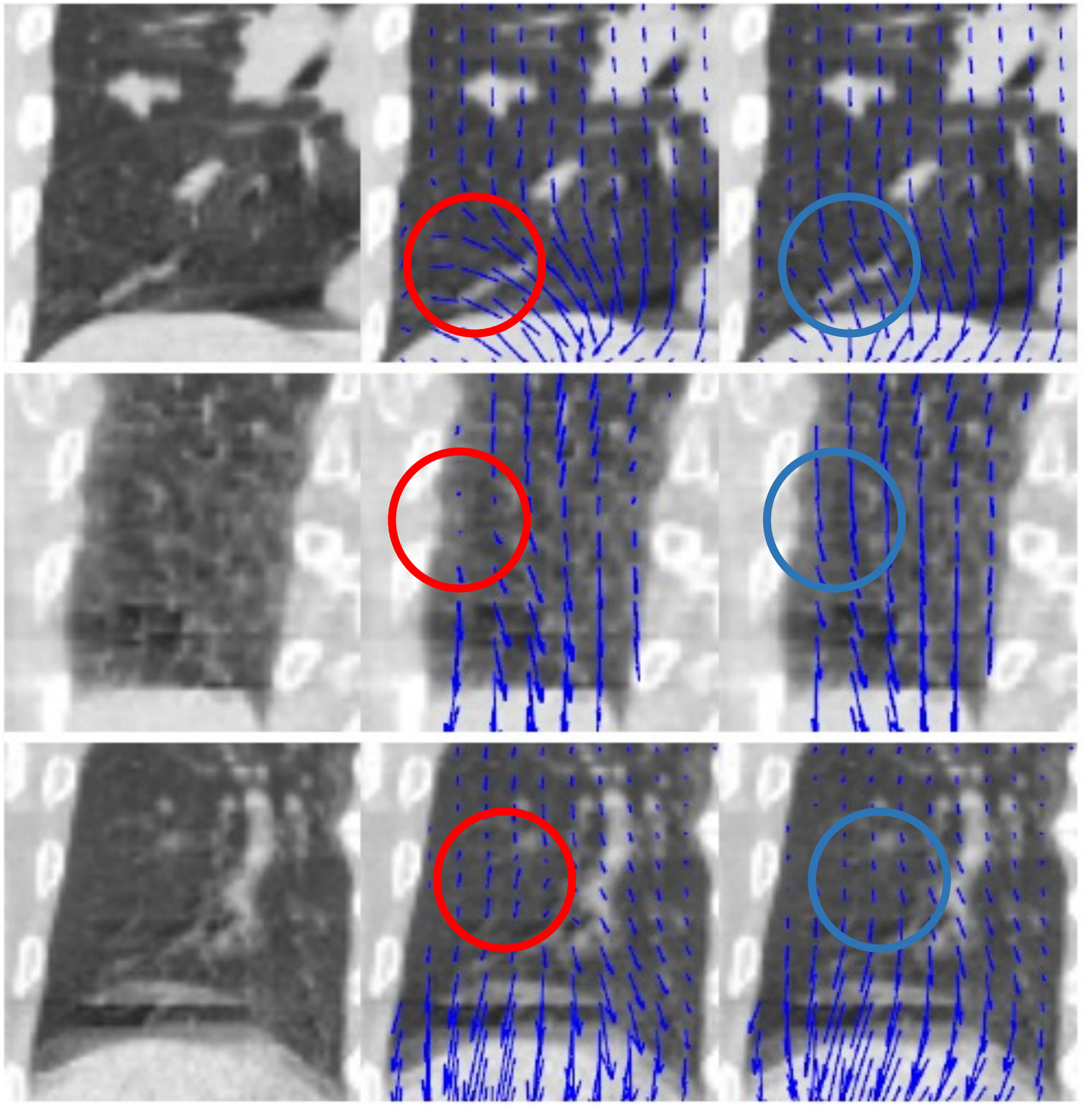

(a) (b) (c)

Summary

- 3D-to-4D spatio-temporal model using cyclic trajectory model
- Piecewise smooth trajectory to account for end-inhale
- Cubic B-splines with control point spacing of 2 or 2.5 frames (for 10 phases) = 5 DOF, while TRE remains within 0.1 mm

- Spatio-temporal registration improves **robustness** to artifacts

[Vandemeulebroucke et al. Med Phys 2011]

- Still long computation time ! ~ twice the time of 9 3D registrations, about 10 hours